Journal of Genetics and Genomics 49 (2022) 85–88

Contents lists available at ScienceDirect

Journal of Genetics and Genomics

Journal homepage: www.journals.elsevier.com/journal-of-genetics-and-genomics/

Letter to the editor

Zfp281 is essential for epiblast maturation through a cell autonomous effect

Pluripotency is recognized as a spectrum of cellular states spanning the naïve pluripotency established in the preimplantation blastocyst and its transition into primed pluripotency in the postimplantation epiblast cells. The exit from pluripotency is followed by the initiation of gastrulation (Brennan et al., 2001; Nichols and Smith, 2009). Naive to primed pluripotent state transition is essential for cell fate decisions, establishing the correct body plan during mammalian embryo development. Zfp281 is a transcription factor known for its critical role in regulating embryonic stem cell (ESC) pluripotency by promoting the naïve to primed pluripotent state transition from our *in vitro* studies of ESCs and epiblast stem cells (EpiSCs) (Fidalgo et al., 2011, 2012; Huang et al., 2017). Our previous work using a global null allele to generate the conventional knockout mouse model also confirmed a key role of *Zfp281* in the epiblast lineage of the developing embryo, manifested by embryonic lethality due to a failure in epiblast maturation (Huang et al., 2017). *Zfp281* is expressed in the pluripotent epiblast and its derivatives and directs the activation of target genes in lineage specification and embryo development. Mechanistically, *Zfp281* cooperates with epigenetic regulators at targeted gene promotors and enhancers to transcriptionally regulate the expression of Nodal signaling pathway genes. *Zfp281* global loss leads to defects in the anterior-posterior (A-P) specification during epiblast maturation (Huang et al., 2017).

In developmental biology, a cell autonomous effect is the property conferred to a type of cells by the cells' own genetic alteration. However, the phenotypic effects in one type of cells (e.g., epiblast) could also be attributed to the same genetic alteration in neighboring cells (e.g., trophectoderm [TE] or primitive endoderm [PrE]) through a non-cell autonomous effect, that is, through direct cell-cell interactions or changes in cell microenvironment or signaling events. As *Zfp281* is also expressed in TE and PrE cells (Huang et al., 2017), it is still unclear whether the defects of epiblast maturation in *Zfp281* mutant embryo are due to a cell autonomous effect of *Zfp281* ablation in epiblast or a non-cell autonomous effect of *Zfp281* ablation in the extraembryonic tissues. We generated tetraploid (4N) chimeric embryos with wildtype 4N TE and PrE and diploid (2N) *Zfp281*KO ESCs and demonstrated that the epiblast-specific loss of *Zfp281* produced embryos with a comparable phenotype to that of *Zfp281* holo-mutant embryos (Huang et al., 2017). However, it is important to note that while the 4N experiment has its unique advantages of being straightforward and timesaving in addressing cell autonomous versus non-cell autonomous effects, it has the limitations of being indirect evidence in an artificial developmental setting, if not technically demanding, because the functional (2N) TE and PrE are also critical for early development. It is known TE cells are committed to the development of placenta, whereas PrE cells are capable of forming the outer layers of the yolk sac, which contribute to the proper embryo development (Tanaka et al., 2009). To unambiguously address this question, we aimed to generate a *Zfp281* conditional knockout (cKO) mouse strain by CRISPR/Cas9 and *Cre/loxP* systems. To construct the *Zfp281* conditional allele, we used the "two-donor floxing method" (Fig. 1A), which uses two sgRNAs and two single-stranded oligonucleotides (ssODNs) containing 34 bp *loxP* sites to flank a targeted critical exon (Yang et al., 2013; Gurumurthy et al., 2019). *Zfp281* gene has a unique 2-exon structure with the Exon2 coding for the full-length protein (Figs. 1A and S1) and the Intron1 containing highly GC-rich sequence, presenting a potential challenge for the *loxP* insertion. Accordingly, we knocked in one *loxP* site (*loxP1*) at Intron1 and a second *loxP* site (*loxP2*) at the position immediately downstream of the stop codon to minimize the possible disruption of 3′ UTR (Figs. 1A and S1). We designed sgRNAs and the donor ssODNs with the *loxP* sequence flanked with 60 bp of homologous arms (Fig. S1). To facilitate the detection of correct targeting, each ssODN was engineered to contain a *Bam*H I restriction site (Figs. 1A and S1B). The Cas9 mRNA, sgRNAs, and ssODNs were injected into 150 zygotes, and the *in vitro* developed blastocysts were then transplanted into the uterus of pseudopregnant females to generate CRISPR founder mice. We obtained 23 (out of 150 or 15.3%) founder pups in total, followed by genotyping of mouse tails through next-generation sequencing. Four of 23 (17.4%) mice contained both *loxP* insertions at the same allele (summarized in Fig. 1B), and the knock-in sequence was confirmed with correctly targeted insertions (Fig. S2A). Our success rate of correct founders (17.4%) is similar to that in a previous report (16%) (Yang et al., 2013). We backcrossed the four founder mice with WT C57BL/6 mice to transmit and segregate the KI allele among the F1 $Zfp281^{F/+}$ mice, then intercrossed the $Zfp281^{F/+}$ male and female mice to obtain the homozygous $Zfp281^{F/F}$ mice (Fig. 1C and 1D). The correct integration of *loxP* sites was further confirmed by Sanger sequencing. The adult $Zfp281^{F/F}$ mice were normal in body weight and fertility compared with the WT C57BL/6 mice (Fig. 1D; Table S1). Thus, we successfully generated the first *Zfp281* cKO mouse model by overcoming the potential *loxP* insertion hurdle associated with the unique 2-exon structure and the GC-rich Intron 1 of the *Zfp281* gene.

To create epiblast-specific KO of *Zfp281*, we bred the $Zfp281^{F/F}$ mice with *Mox2-Cre* (heterozygous, $Mox2^{Cre/+}$) mice (Tallquist and Soriano, 2000) (kind gift from Dr. Soriano in Mt. Sinai), which expresses the *Cre* recombinase from the endogenous *Mox2* locus. This *Mox2-Cre* line drives the expression of *Cre* throughout the epiblast and its derivatives following implantation as early as E5.0 (Tallquist and Soriano, 2000). By crossing the $Zfp281^{F/F}$ and $Mox2^{Cre/+}$ mice (Fig. 1C), we expected to achieve epiblast-specific deletion of *Zfp281* in early mouse embryos. We obtained two genotypes in the pups following this mating

https://doi.org/10.1016/j.jgg.2021.08.016

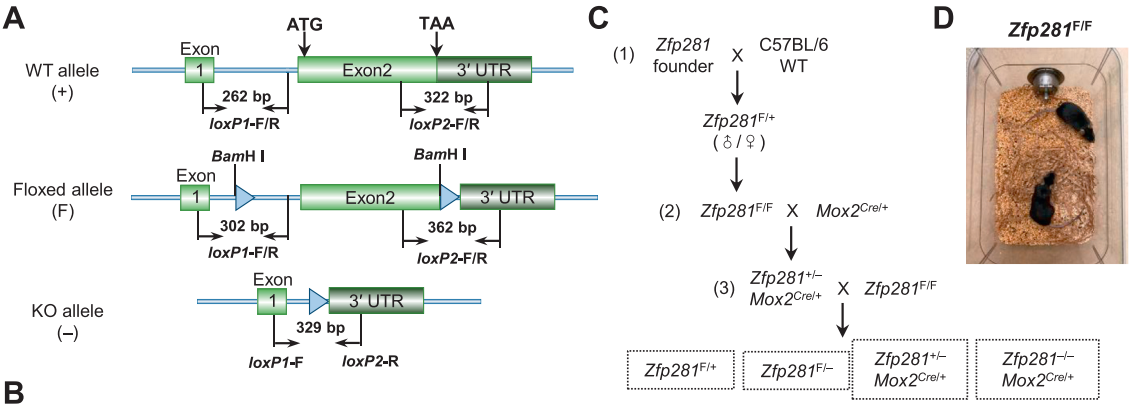

B

Target site	Embryos injected	Live pups born	Non-transgenic	Targeted *loxP2*	Targeted *loxP1* + *loxP2*
Zfp281 Exon2	150	23 (15.3%)	13/23 (56.5%)	7/23 (30.43%)	4/23 (17.4%)

E

Mating strategy	Litter size	Offspring genotype			
		Zfp281$^{F/+}$	*Zfp281*$^{F/–}$	*Zfp281*$^{+/–}$ *Mox2*$^{Cre/+}$	*Zfp281*$^{–/–}$ *Mox2*$^{Cre/+}$
Zfp281$^{+/–}$ *Mox2*$^{Cre/+}$ X *Zfp281*$^{F/F}$	4	1	2	1	0
	5	2	2	1	0
	6	4	0	2	0
	7	4	1	2	0
	4	2	1	1	0
	5	1	2	2	0
	4	2	1	1	0
	6	2	2	2	0
	6	2	2	2	0
Total	47	20 (42.6%)	13 (27.6%)	14 (29.8%)	0 (0%)

F

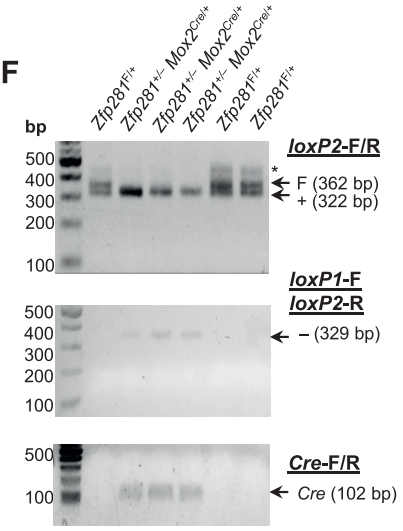

G

Mating strategy	Litter size	E6.5~E7.5 embryos genotype				
		Zfp281$^{F/+}$	*Zfp281*$^{F/–}$	*Zfp281*$^{+/–}$ *Mox2*$^{Cre/+}$	*Zfp281*$^{–/–}$ *Mox2*$^{Cre/+}$	N/A
Zfp281$^{+/–}$ *Mox2*$^{Cre/+}$ X *Zfp281*$^{F/F}$	9	3	2	2	1	1
	9	1	3	1	2	2
Total	18	4 (22.2%)	5 (27.8%)	3 (16.7%)	3 (16.7%)	3 (16.7%)

H

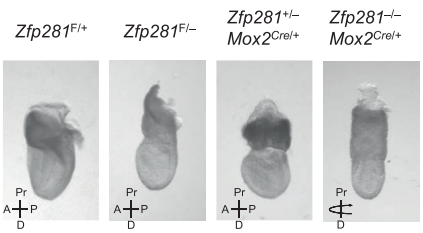

Fig. 1. Generation of an epiblast-specific *Zfp281* conditional knockout (cKO) mouse strain and confirmation of *Zfp281* KO lethality through a cell autonomous effect. **A**: Schematic depiction of the generation of *Zfp281* cKO allele. The *Zfp281* exons, intron, 3′ UTR, the start (ATG) and stop (TAA) codons, the knock-in *Bam*H I restriction sites and two *loxP* sites, and the primers used for genotyping are labeled. **B**: Statistics of *loxP* insertion at two sites of the *Zfp281* locus using CRISPR/Cas9 targeting in *in vitro* developed blastocysts and the targeted live pups (founder mice). **C**: Schematic depiction of breeding strategy to generate desired genotypes in mice. (1) The *Zfp281* founder mice (usually mosaic) were backcrossed with WT C57BL/6 mice to transmit and segregate the *Zfp281 loxP* allele, then the heterozygous (*Zfp281*$^{F/+}$) mice were intercrossed to obtain the homozygous (*Zfp281*$^{F/F}$) mice; (2) The *Zfp281*$^{F/F}$ and *Mox2*$^{Cre/+}$ mice were bred to transmit the *loxP* allele with the *Cre* recombinase to obtain the *Zfp281*$^{+/–}$*Mox2*$^{Cre/+}$ mouse strain; (3) *Zfp281*$^{+/–}$*Mox2*$^{Cre/+}$ and *Zfp281*$^{F/F}$ mice were bred to generate four theoretical genotypes of the pups. **D**: *Zfp281*$^{F/F}$ adult mice used in this study. The identity of these mice was confirmed by genotyping and sequencing. **E**: Statistics of the genotyping result of live pups by mating *Zfp281*$^{F/F}$ and *Zfp281*$^{+/–}$*Mox2*$^{Cre/+}$ mice. **F**: Examples of genotyping PCR results showing different alleles. * indicates the potential hybrid DNA of amplified Flox and wildtype bands. **G**: Statistics of the genotyping result of dissected embryos by mating *Zfp281*$^{F/F}$ and *Zfp281*$^{+/–}$*Mox2*$^{Cre/+}$ mice. N/A means genotyping is not successful because of very limited materials. **H**: Epiblast-specific *Zfp281* cKO embryo (*Zfp281*$^{–/–}$*Mox2*$^{Cre/+}$) exhibits abnormal morphology at E7.0, compared with the other (*Zfp281*$^{F/+}$, *Zfp281*$^{F/–}$, and *Zfp281*$^{+/–}$*Mox2*$^{Cre/+}$) littermates. A, anterior; P, posterior; Pr, proximal; D, distal.

strategy, *Zfp281*$^{F/+}$(*Mox2*$^{+/+}$) and *Zfp281*$^{+/-}$*Mox2*$^{Cre/+}$, confirmed by genotyping PCR (Fig. 1F; PCR primers shown in Fig. 1A, see details in Table S2). This result confirms that the *Mox2-Cre* line works well with the *Zfp281* floxed allele, resulting in the *Mox2-Cre* excised *Zfp281* null allele. We further mated *Zfp281*$^{+/-}$*Mox2*$^{Cre/+}$ mice with the *Zfp281*$^{F/F}$ mice (Fig. 1C), which would theoretically generate pups of four genotypes, *Zfp281*$^{F/+}$(*Mox2*$^{+/+}$), *Zfp281*$^{F/-}$(*Mox2*$^{+/+}$), *Zfp281*$^{+/-}$*Mox2*$^{Cre/+}$, and *Zfp281*$^{-/-}$*Mox2*$^{Cre/+}$, with an expected ratio of 1:1:1:1. Because *Mox2* is only expressed in the epiblast and its derivatives, the *Zfp281*$^{-/-}$*Mox2*$^{Cre/+}$ embryos should have an epiblast-specific deletion of *Zfp281*, whereas embryos with the other three genotypes should have at least one allele with normal Zfp281 protein expression. Of note, because *Mox2* is not expressed in extraembryonic tissues, the extraembryonic lineages should be either *Zfp281*$^{F/+}$ or *Zfp281*$^{F/-}$ genotype, with at least one allele of normal Zfp281 protein expression. With this mating strategy, we obtained a total of 47 pups from 9 litters (an average of 5.2 pups per litter). By PCR genotyping, we obtained 20 (42.6%), 13 (27.6%), and 14 (29.8%) pups with *Zfp281*$^{F/+}$, *Zfp281*$^{F/-}$, and *Zfp281*$^{+/-}$*Mox2*$^{Cre/+}$ genotypes, respectively (summarized in Fig. 1E; part of the genotyping result is shown in Fig. S2B and S2C), but zero *Zfp281*$^{-/-}$*Mox2*$^{Cre/+}$ pups. Our results demonstrate that the epiblast-specific deletion of *Zfp281* in the *Zfp281*$^{-/-}$*Mox2*$^{Cre/+}$ embryos is embryonic lethal, which is consistent with the *Zfp281* conventional KO results in our previous study (Huang et al., 2017). This study thus confirms that *Zfp281* is essential for mouse embryo development, and importantly, conclusively demonstrates a cell autonomous effect of Zfp281 in epiblast development.

Vertebrates have three principal body axes: the anterior-posterior (A-P), the dorsal-ventral (D-V), and the left-right (L-R) axes. The A-P axis is the first established and morphologically discernible axis of the body during mouse embryo development. During early postimplantation embryo development (E4.5 to E6.5), the distal visceral endoderm, a subpopulation of PrE, forms at the distal tip of the embryo, migrates to the future anterior side, and derives signals to induce the head structures on the nearby epiblast (Tam and Loebel, 2007). Nodal, as well as several of its pathway components, such as Lefty1, Cripto, Dkk1, and Foxh1, are essential for A-P axis establishment (Ding et al., 1998; Brennan et al., 2001; Yamamoto et al., 2001; Kimura-Yoshida et al., 2005). We previously showed that *Zfp281* mutant embryos display indistinguishable A-P axis, compared with the WT littermates as early as E6.0–6.5 (Huang et al., 2017). To determine whether the embryos with the epiblast-specific *Zfp281* deletion phenocopy the defects of conventional *Zfp281* mutant embryos in early development, we dissected the embryos at early postimplantation stages (E6.5–7.5) after crossing the *Zfp281*$^{+/-}$*Mox2*$^{Cre/+}$ and *Zfp281*$^{F/F}$ mice (Fig. 1C). The *Zfp281*$^{-/-}$*Mox2*$^{Cre/+}$ embryos were identified by abnormal morphology, including A-P symmetry and shrunken epiblast, which was further confirmed by PCR genotyping (summarized in Fig. 1G, typical embryos of each genotype are shown in Fig. 1H). In contrast, all the embryos with the other three genotypes (*Zfp281*$^{F/+}$, *Zfp281*$^{F/-}$, and *Zfp281*$^{+/-}$*Mox2*$^{Cre/+}$) were normally developed. These results demonstrate that epiblast-specific deletion of *Zfp281* phenocopies the failure of *Zfp281* conventional KO mutant in epiblast maturation during early embryo development.

In conclusion, we established a conditional *Zfp281* KO mouse model and, combined with epiblast-specific *Cre* excision, demonstrated conclusively a cell autonomous effect of *Zfp281* functions in mouse embryo development. This novel *Zfp281* conditional KO mouse strain will also be a valuable resource to investigate other tissue-specific functions of *Zfp281* in development and disease in the future.

Conflict of interest

The authors declare no conflict of interest.

Acknowledgments

We thank Dr. Philippe Soriano for providing the *Mox2-Cre* mice. Research in the Wang laboratory was funded by grants from the National Institutes of Health (R01GM129157, R01HD095938, R01HD097268, and R01HL146664) and by contracts from New York State Stem Cell Science (NYSTEM#C35583GG and C35584GG). R.Z. was a visiting student at Columbia University Irving Medical Center sponsored by the China Scholarship Council.

Supplementary data

Supplementary data to this article can be found online at https://doi.org/10.1016/j.jgg.2021.08.016.

References

Brennan, J., Lu, C.C., Norris, D.P., Rodriguez, T.A., Beddington, R.S., Robertson, E.J., 2001. Nodal signalling in the epiblast patterns the early mouse embryo. Nature 411, 965–969.

Ding, J., Yang, L., Yan, Y.T., Chen, A., Desai, N., Wynshaw-Boris, A., Shen, M.M., 1998. Cripto is required for correct orientation of the anterior-posterior axis in the mouse embryo. Nature 395, 702–707.

Fidalgo, M., Faiola, F., Pereira, C.F., Ding, J., Saunders, A., Gingold, J., Schaniel, C., Lemischka, I.R., Silva, J.C., Wang, J., 2012. Zfp281 mediates Nanog autorepression through recruitment of the NuRD complex and inhibits somatic cell reprogramming. Proc. Natl. Acad. Sci. U. S. A. 109, 16202–16207.

Fidalgo, M., Shekar, P.C., Ang, Y.S., Fujiwara, Y., Orkin, S.H., Wang, J., 2011. Zfp281 functions as a transcriptional repressor for pluripotency of mouse embryonic stem cells. Stem Cell. 29, 1705–1716.

Gurumurthy, C.B., O'Brien, A.R., Quadros, R.M., Adams Jr., J., Alcaide, P., Ayabe, S., Ballard, J., Batra, S.K., Beauchamp, M.C., Becker, K.A., et al., 2019. Reproducibility of CRISPR-Cas9 methods for generation of conditional mouse alleles: a multi-center evaluation. Genome Biol. 20, 171.

Huang, X., Balmer, S., Yang, F., Fidalgo, M., Li, D., Guallar, D., Hadjantonakis, A.K., Wang, J., 2017. Zfp281 is essential for mouse epiblast maturation through transcriptional and epigenetic control of Nodal signaling. eLife 6, e33333.

Kimura-Yoshida, C., Nakano, H., Okamura, D., Nakao, K., Yonemura, S., Belo, J.A., Aizawa, S., Matsui, Y., Matsuo, I., 2005. Canonical Wnt signaling and its antagonist regulate anterior-posterior axis polarization by guiding cell migration in mouse visceral endoderm. Dev. Cell 9, 639–650.

Nichols, J., Smith, A., 2009. Naive and primed pluripotent states. Cell Stem Cell 4, 487–492.

Tallquist, M.D., Soriano, P., 2000. Epiblast-restricted Cre expression in MORE mice: a tool to distinguish embryonic vs. extra-embryonic gene function. Genesis 26, 113–115.

Tam, P.P., Loebel, D.A., 2007. Gene function in mouse embryogenesis: get set for gastrulation. Nat. Rev. Genet. 8, 368–381.

Tanaka, M., Hadjantonakis, A.K., Vintersten, K., Nagy, A., 2009. Aggregation chimeras: combining ES cells, diploid, and tetraploid embryos. Methods Mol. Biol. 530, 287–309.

Yamamoto, M., Meno, C., Sakai, Y., Shiratori, H., Mochida, K., Ikawa, Y., Saijoh, Y., Hamada, H., 2001. The transcription factor FoxH1 (FAST) mediates Nodal signaling during anterior-posterior patterning and node formation in the mouse. Gene Dev. 15, 1242–1256.
Yang, H., Wang, H., Shivalila, C.S., Cheng, A.W., Shi, L., Jaenisch, R., 2013. One-step generation of mice carrying reporter and conditional alleles by CRISPR/Cas-mediated genome engineering. Cell 154, 1370–1379.

Ruge Zang
Clinical and Translational Research Center of Shanghai First Maternity and Infant Hospital, School of Life Sciences and Technology, Tongji University, Shanghai 200092, China

Department of Medicine, Columbia Center for Human Development, Columbia Stem Cell Initiative, Herbert Irving Comprehensive Cancer Center, Columbia University Irving Medical Center, New York, NY 10032, USA

Xin Huang, Dan Li, Hongwei Zhou
Department of Medicine, Columbia Center for Human Development, Columbia Stem Cell Initiative, Herbert Irving Comprehensive Cancer Center, Columbia University Irving Medical Center, New York, NY 10032, USA

Shaorong Gao
Clinical and Translational Research Center of Shanghai First Maternity and Infant Hospital, School of Life Sciences and Technology, Tongji University, Shanghai 200092, China

Jianlong Wang*
Department of Medicine, Columbia Center for Human Development, Columbia Stem Cell Initiative, Herbert Irving Comprehensive Cancer Center, Columbia University Irving Medical Center, New York, NY 10032, USA

* Corresponding author.
E-mail address: jw3925@cumc.columbia.edu (J. Wang).

14 July 2021
Available online 17 September 2021